

Exciton-phonon resonance in the continuum absorption of bulk semiconductors

R. Zimmermann

Institut für Physik der Humboldt-Universität zu Berlin, Hausvogteiplatz 5-7, D-10117 Berlin, Federal Republic of Germany

C. Trallero-Giner

Department of Theoretical Physics, Havana University, Vedado 10400, Havana, Cuba

(Received 22 May 1997)

In polar semiconductors, resonances occur due to the interaction of excitonic states (discrete and continuous) with excitations involving virtual excitons plus a longitudinal-optical (LO) phonon. A theory is presented which starts with bare electrons, holes, and phonons, interacting via Coulomb attraction and Fröhlich coupling. Within a self-consistent one-phonon treatment, a nonlinear and nonlocal Schrödinger equation for the exciton Green's function is derived. Only after extracting a Haken type effective potential as zeroth-order, perturbation theory with respect to the dynamical nature of the exciton-phonon interaction can be applied. Accurate measurements of the exciton absorption continuum in CdTe and, recently, in GaAs display around the resonance energy a slight change of slope which can be quantitatively explained by the present exciton-phonon model. For GaAs, first-order perturbation theory with respect to exciton-LO-phonon coupling is found sufficient, whereas for CdTe, a full solution of the nonlocal exciton equation is necessary. [S0163-1829(97)07739-4]

I. INTRODUCTION

A peculiar weak feature in the excitonic continuum has been observed in several optical experiments with bulk semiconductors which appears at approximately one-longitudinal-optical- (LO-) phonon energy above the exciton line. We mention absorption measurements in ionic crystals as ZnO,¹ MgO, and BeO,² reflectivity and transmission experiments on CdS, CdSe, and CdTe,^{3,4} low temperature laser-excited photoemission of InP,⁵ CdTe, Cd_xZn_{1-x}Te and *n*-type CdTe:I epilayers,⁶ and an ellipsometric study of Zn_xCd_{1-x}Se⁷ among the different systems and experimental configurations. In GaAs, differential transmission spectra with femtosecond time resolution⁸ and high-resolution absorption spectra⁹ have been reported recently. In all these cases a clear experimental deviation from the standard (phonon-free) Elliott theory¹⁰ has been seen and related to the exciton-LO-phonon coupling. The observed structure was assigned to a resonance due to the interaction of excitonic states (discrete and continuous) with excitations involving virtual excitons plus one LO phonon. On the theoretical side, an exciton-phonon complex for the 2*s* state was constructed using a variational method and single-phonon 1*s*-2*s* coupling in Ref. 11. The same treatment for *p*-states was given in Ref. 12. In both cases the exciton binding energy is assumed to be close to the LO-phonon energy. A generalization to exciton continuum states has been elaborated by Sak¹³ using first-order perturbation theory for the exciton Green's function.

In this paper we derive a theoretical description for the optical response including the exciton-phonon resonance (XPR) which goes beyond perturbation theory. It is shown that the inclusion of polaron effects in the form of Haken's potential¹⁴ is crucial for a correct description of the exciton absorption in polar semiconductors. In this way earlier attempts using plain perturbation theory¹³ or assuming a diagonal self-energy¹⁵ are substantially improved.

The outline of the paper is as follows. In Sec. II, the concept of the exciton Green's function is introduced, and basic relations are given to evaluate the linear optical response. The exciton-phonon problem is outlined in Sec. III, starting with a Hamiltonian for electrons, holes, and LO phonons interacting via the bare Coulomb potential and the Fröhlich coupling. In Sec. IV a one-phonon treatment is established and improved using diagrammatic arguments, ending up with a self-consistent Schrödinger equation for the exciton Green's function. In Sec. V a modified static Haken potential is derived which serves as a starting point for investigating the dynamical aspect of the exciton-phonon coupling. Results for CdTe and GaAs are presented in Sec. VI and compared with available experimental data. The numerical procedure used for calculating the exciton Green's function is described in the Appendix.

II. GREEN'S FUNCTION FOR EXCITON SPECTRA

In electron-hole relative space, the Wannier-Mott exciton is defined as the solution of the three-dimensional Schrödinger equation

$$\left(E_{g0} - \frac{\hbar^2}{2\mu} \Delta_{\mathbf{r}} - \frac{e^2}{\epsilon_0 r} \right) \phi_n(\mathbf{r}) = \mathcal{E}_n \phi_n(\mathbf{r}), \quad (1)$$

where μ is the reduced effective mass ($\mu^{-1} = m_e^{-1} + m_h^{-1}$), m_e (m_h) the bare electron (hole) band mass, ϵ_0 the static dielectric constant, E_{g0} the direct energy gap at the Γ point, and $\phi_n(\mathbf{r})$ the internal exciton wave function of the n th state with energy \mathcal{E}_n .

Dropping a prefactor which includes, e.g., the interband momentum matrix element, the absorption at frequency ω is related to the imaginary part of the linear optical response,

$$\text{Im } \chi(\omega) = \sum_n |\phi_n(\mathbf{r}=0)|^2 \pi \delta(\hbar\omega - \mathcal{E}_n), \quad (2)$$

and consists of a sum over bound states at $\mathcal{E}_n = E_{g0} - R_0/n^2$ and the Sommerfeld-enhanced continuum,¹⁰

$$\text{Im } \chi(\omega) \sim \sum_{n=1}^{\infty} \frac{2}{n^3} \delta(E + 1/n^2) + \frac{\Theta(E)}{1 - \exp(2\pi/\sqrt{E})}, \quad (3)$$

with $E = (\hbar\omega - E_{g0})/R_0$ and the Heaviside step function $\Theta(E)$. The 1s exciton binding energy equals $R_0 = \mu/\epsilon_0^2 \times 13.6$ eV.

If the exciton continuum is involved, the explicit use of the corresponding scattering wave functions is inconvenient. Easier to handle is the exciton Green's function (or resolvent)

$$G_0(\mathbf{r}, \mathbf{r}', z) = \sum_n \frac{\phi_n^*(\mathbf{r}) \phi_n(\mathbf{r}')}{\mathcal{E}_n - \hbar z} \quad (4)$$

at complex energy $\hbar z = \hbar\omega + i\gamma$. The function G_0 obeys the inhomogeneous exciton Schrödinger equation

$$\left(E_{g0} - \frac{\hbar^2}{2\mu} \Delta_{\mathbf{r}} - \frac{e^2}{\epsilon_0 r} - \hbar z \right) G_0(\mathbf{r}, \mathbf{r}', z) = \delta(\mathbf{r} - \mathbf{r}'), \quad (5)$$

and the optical response including a Lorentz broadening γ follows from

$$\chi(z) = G_0(\mathbf{r} \rightarrow 0, \mathbf{r}' \rightarrow 0, z). \quad (6)$$

The limit has to be taken carefully since the real part of the Green's function diverges at $\mathbf{r} \rightarrow 0$. A proper regularization procedure has been described in Ref. 16. For electron-hole potentials which differ from the simple Coulomb law, no analytic solution is possible. However, the Green's function can be computed very efficiently¹⁶ as outlined in the Appendix.

III. EXCITON-PHONON HAMILTONIAN

We add to the electron-hole Hamiltonian with Coulomb attraction the Fröhlich interaction with (dispersionless) longitudinal-optical phonons of energy $\hbar\omega_0$,

$$\begin{aligned} \mathcal{H} = & E_{g\infty} - \frac{\hbar^2}{2m_e} \Delta_{\mathbf{r}_e} - \frac{\hbar^2}{2m_h} \Delta_{\mathbf{r}_h} - \frac{e^2}{\epsilon_{\infty} |\mathbf{r}_e - \mathbf{r}_h|} \\ & + \sum_{\mathbf{q}} \hbar\omega_0 \left(a_{\mathbf{q}}^{\dagger} a_{\mathbf{q}} + \frac{1}{2} \right) + \sum_{\mathbf{q}} \sqrt{\frac{4\pi e^2 \hbar\omega_0}{\eta q^2}} \frac{1}{2} \\ & \times (e^{i\mathbf{q}\mathbf{r}_e} - e^{i\mathbf{q}\mathbf{r}_h}) (a_{\mathbf{q}}^{\dagger} + a_{-\mathbf{q}}), \end{aligned} \quad (7)$$

where $\eta^{-1} = \epsilon_{\infty}^{-1} - \epsilon_0^{-1}$ determines the strength of the polar coupling, and $a_{\mathbf{q}}^{\dagger}$ ($a_{\mathbf{q}}$) creates (annihilates) a LO phonon at wave vector \mathbf{q} . The electron (hole) position coordinate is denoted by \mathbf{r}_e (\mathbf{r}_h), and a unity normalization volume is assumed. Note that the bare energy gap $E_{g\infty}$ and the electronic background screening constant ϵ_{∞} enter the Hamiltonian. The experimentally relevant energy gap and the full screening contain polaron contributions which follow from the Fröhlich interaction and have to be calculated explicitly as detailed below. We stress this point since earlier investigations of the exciton-phonon resonance were incorrect in this respect.^{13,15}

Introducing relative and center-of-mass (COM) coordinates as

$$\mathbf{r}_e = \mathbf{R} + \frac{m_h}{M} \mathbf{r}, \quad \mathbf{r}_h = \mathbf{R} - \frac{m_e}{M} \mathbf{r}, \quad (8)$$

the Hamiltonian is cast into

$$\mathcal{H} = \mathcal{H}_{\infty} + \sum_{\mathbf{q}} \hbar\omega_0 \left(a_{\mathbf{q}}^{\dagger} a_{\mathbf{q}} + \frac{1}{2} \right) + \sum_{\mathbf{q}} M_{\mathbf{q}}(\mathbf{r}) e^{i\mathbf{q}\mathbf{R}} (a_{\mathbf{q}}^{\dagger} + a_{-\mathbf{q}}). \quad (9)$$

Here, we have defined the phonon-free exciton Hamiltonian \mathcal{H}_{∞} ,

$$\mathcal{H}_{\infty} = E_{g\infty} - \frac{\hbar^2}{2\mu} \Delta_{\mathbf{r}} - \frac{\hbar^2}{2M} \Delta_{\mathbf{R}} - \frac{e^2}{\epsilon_{\infty} r}, \quad (10)$$

with exciton mass $M = m_e + m_h$, and the coupling function $M_{\mathbf{q}}(\mathbf{r})$ is introduced as

$$M_{\mathbf{q}}(\mathbf{r}) = \sqrt{\frac{4\pi e^2 \hbar\omega_0}{\eta q^2}} \frac{1}{2} (e^{i\mathbf{q}\mathbf{r}m_h/M} - e^{-i\mathbf{q}\mathbf{r}m_e/M}). \quad (11)$$

The corresponding exciton Green's function \hat{G} of the Hamiltonian (9) is defined as a resolvent operator of the equation

$$(\mathcal{H} - \hbar z) \hat{G} = \hat{1}, \quad (12)$$

and the optical response function can be expressed as

$$\chi(z) = \int d\mathbf{R} d\mathbf{R}' \langle 0 | \hat{G}(\mathbf{r}=0, \mathbf{R}, \mathbf{r}'=0, \mathbf{R}', z) | 0 \rangle. \quad (13)$$

Since we are interested in the linear response or optical dielectric function at zero temperature, we have to project onto the phonon vacuum state $|0\rangle$. From Eq. (12) follows that the function

$$|\hat{\Psi}(\mathbf{r}, \mathbf{R}, z)\rangle = \int d\mathbf{R}' \hat{G}(\mathbf{r}, \mathbf{R}, \mathbf{r}'=0, \mathbf{R}', z) |0\rangle \quad (14)$$

is the solution of

$$(\mathcal{H} - \hbar z) |\hat{\Psi}(\mathbf{r}, \mathbf{R}, z)\rangle = \delta(\mathbf{r}) |0\rangle, \quad (15)$$

and gives the response function directly as

$$\chi(z) = \int d\mathbf{R} \langle 0 | \hat{\Psi}(\mathbf{r}=0, \mathbf{R}, z) \rangle. \quad (16)$$

IV. SELF-CONSISTENT ONE-PHONON TREATMENT

If written in a phonon number representation, Eq. (15) forms an infinite hierarchy of equations where each n -phonon state is coupled to $(n+1)$ and $(n-1)$. As the main approximation being valid for moderate exciton-phonon coupling we restrict ourselves to the subspace of zero- and one-phonon states only, that is¹⁷

$$|\hat{\Psi}(\mathbf{r}, \mathbf{R}, z)\rangle = \Psi^{(0)}(\mathbf{r}, \mathbf{R}, z) |0\rangle + \sum_{\mathbf{q}} \Psi_{\mathbf{q}}^{(1)}(\mathbf{r}, \mathbf{R}, z) a_{\mathbf{q}}^{\dagger} |0\rangle, \quad (17)$$

where $\Psi^{(0)}$ ($\Psi_q^{(1)}$) is the zero- (one-) LO-phonon exciton wave function. Using the above expression for $|\hat{\Psi}\rangle$ and Eqs. (9) and (15), we obtain only two coupled equations

$$(\mathcal{H}_\infty - \hbar z)\Psi^{(0)}(\mathbf{r}, \mathbf{R}, z) + \sum_{\mathbf{q}} M_{\mathbf{q}}^*(\mathbf{r}) e^{-i\mathbf{q}\mathbf{R}} \Psi_q^{(1)}(\mathbf{r}, \mathbf{R}, z) = \delta(\mathbf{r}), \quad (18)$$

$$(\hbar\omega_0 + \mathcal{H}_\infty - \hbar z)\Psi_q^{(1)}(\mathbf{r}, \mathbf{R}, z) + M_{\mathbf{q}}(\mathbf{r}) e^{i\mathbf{q}\mathbf{R}} \Psi^{(0)}(\mathbf{r}, \mathbf{R}, z) = 0, \quad (19)$$

which can be solved as follows. The bare exciton Green's function $G_\infty(\mathbf{r}, \mathbf{R}, \mathbf{r}', \mathbf{R}', z)$ satisfies the equation

$$(\mathcal{H}_\infty - \hbar z)G_\infty(\mathbf{r}, \mathbf{R}, \mathbf{r}', \mathbf{R}', z) = \delta(\mathbf{r} - \mathbf{r}') \delta(\mathbf{R} - \mathbf{R}'). \quad (20)$$

Hence, Eq. (19) can be solved as

$$\Psi_q^{(1)}(\mathbf{r}, \mathbf{R}, z) = - \int d\mathbf{r}' d\mathbf{R}' G_\infty(\mathbf{r}, \mathbf{R}, \mathbf{r}', \mathbf{R}', z - \omega_0) M_{\mathbf{q}}(\mathbf{r}') \times e^{i\mathbf{q}\mathbf{R}'} \Psi^{(0)}(\mathbf{r}', \mathbf{R}', z) \quad (21)$$

and inserted into Eq. (18) to form a closed equation for the zero-phonon exciton wave function.

Since we have assumed a parabolic dispersion for electrons and holes, the COM motion factorizes as a plane wave with the kinetic exciton energy $\epsilon_{\mathbf{Q}} \equiv \hbar\omega_{\mathbf{Q}} = \hbar^2 Q^2 / 2M$. Consequently, the bare Green's function can be written in the form

$$G_\infty(\mathbf{r}, \mathbf{R}, \mathbf{r}', \mathbf{R}', z) = \sum_{\mathbf{Q}} e^{i\mathbf{Q}(\mathbf{R} - \mathbf{R}')} G_\infty(\mathbf{r}, \mathbf{r}', z - \omega_{\mathbf{Q}}), \quad (22)$$

where the right-hand side Green's function acts in relative space only. For the optical response, we need $\mathbf{Q} = 0$ only (long-wave limit of the light field). Therefore, $\Psi^{(0)}(\mathbf{r}, \mathbf{R}, z)$ can be taken independent of \mathbf{R} , and using Eqs. (18), (21), and (22), we end up with

$$\left(E_{g_\infty} - \frac{\hbar^2}{2\mu} \Delta_{\mathbf{r}} - \frac{e^2}{\epsilon_\infty r} - \hbar z \right) \Psi^{(0)}(\mathbf{r}, z) - \sum_{\mathbf{q}} \int d\mathbf{r}' M_{\mathbf{q}}^*(\mathbf{r}) G_\infty(\mathbf{r}, \mathbf{r}', z - \omega_0 - \omega_{\mathbf{q}}) M_{\mathbf{q}}(\mathbf{r}') \times \Psi^{(0)}(\mathbf{r}', z) = \delta(\mathbf{r}). \quad (23)$$

The response is now simply given by

$$\chi(z) = \Psi^{(0)}(\mathbf{r} = 0, z). \quad (24)$$

Without exciton-phonon interaction, the solution of Eq. (23) would be $\Psi^{(0)}(\mathbf{r}, z) = G_\infty(\mathbf{r}, \mathbf{r}' = 0, z)$. Figure 1(a) shows the diagrammatic Dyson equation for the exciton Green's function $G(\mathbf{r}, \mathbf{r}', z)$ of Eq. (23). Note that in the coupling term the *bare* Green's function $G_\infty(\mathbf{r}, \mathbf{r}', z)$ enters. This inconsistency can be cured by adding further diagrams to the Dyson equation of Fig. 1(a). Then, all Green's functions refer to the same level of approximation. Technically, G_∞ in Eq. (23) has to be replaced by the full Green's function G ,

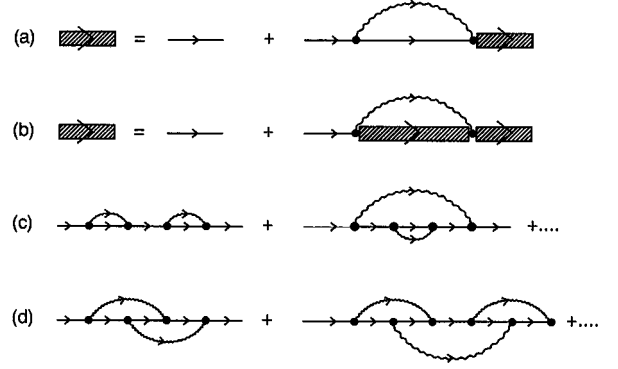


FIG. 1. (a) Diagrammatic Dyson equation for the exciton Green's function G (hatched block) given by Eq. (23). The LO-phonon propagator is depicted as wavy line, and the self-energy contains the bare exciton Green's function G_∞ (thin line). (b) Diagrammatic form of the improved Dyson equation (25) where G_∞ is replaced by the full Green's function G in the self-energy. (c) Second-order diagrams taken into account to get the Dyson equation (b). (d) Crossed diagrams which are not included in the Dyson equation (b).

$$\left(E_{g_\infty} - \frac{\hbar^2}{2\mu} \Delta_{\mathbf{r}} - \frac{e^2}{\epsilon_\infty r} - \hbar z \right) G(\mathbf{r}, \mathbf{r}', z) - \sum_{\mathbf{q}} \int d\mathbf{r}' M_{\mathbf{q}}^*(\mathbf{r}) G(\mathbf{r}, \mathbf{r}', z - \omega_0 - \omega_{\mathbf{q}}) M_{\mathbf{q}}(\mathbf{r}') \times G(\mathbf{r}', \mathbf{r}'', z) = \delta(\mathbf{r} - \mathbf{r}''). \quad (25)$$

The second diagram in Fig. 1(c) is the lowest-order nested diagram, the sequence of which has to be summed up to convert the Dyson equation of Fig. 1(a) into Fig. 1(b) [or Eq. (25)]. Crossing-type diagrams [Fig. 1(d)] are not included here. They would play the role of vertex corrections.¹⁸

The nonlinear and nonlocal integral equation (25) is called a self-consistent one-phonon approximation. It is exactly the self-consistent treatment which places the exciton-phonon resonance at the correct energetic position: If G has a pole at the exciton energy \mathcal{E}_n which includes the polar interaction, then the self-energy term [sum over \mathbf{q} in Eq. (25)] exhibits a singularity just at $\mathcal{E}_n + \hbar\omega_0$.

V. PERTURBATION AROUND THE HAKEN POTENTIAL

For a weakly polar material and, in particular, if the exciton binding energy is small with respect to the phonon energy, \mathcal{H}_∞ is not a good start for perturbation theory. To derive an effective electron-hole interaction which includes already some part of the polar interaction, we use the large-frequency limit of the Green's function,

$$G(\mathbf{r}, \mathbf{r}', z) \rightarrow \frac{\delta(\mathbf{r} - \mathbf{r}')}{-\hbar z}, \quad (26)$$

in the self-energy term of Eq. (25) which gives the local equation,

$$\left(E_{g\infty} - \frac{\hbar^2}{2\mu} \Delta_{\mathbf{r}} - \frac{e^2}{\epsilon_{\infty} r} - \hbar z - \sum_{\mathbf{q}} \frac{|M_{\mathbf{q}}(\mathbf{r})|^2}{\hbar \omega_0 + \epsilon_{\mathbf{q}}} \right) G_H(\mathbf{r}, \mathbf{r}'', z) = \delta(\mathbf{r} - \mathbf{r}''). \quad (27)$$

The additional term is

$$- \sum_{\mathbf{q}} \frac{|M_{\mathbf{q}}(\mathbf{r})|^2}{\hbar \omega_0 + \epsilon_{\mathbf{q}}} = \frac{e^2}{\eta r} (1 - r/r_0 - e^{-r/r_0}), \quad (28)$$

with the polaron radius $r_0^2 = \hbar/(2M\omega_0)$. Equation (28) contains a constant part which forms the polaron shift of the bare gap,

$$E_{g0} = E_{g\infty} - e^2/(\eta r_0). \quad (29)$$

The r -dependent terms can be combined with the ϵ_{∞} -screened Coulomb potential into

$$V_H(r) = -\frac{e^2}{r} [\epsilon_0^{-1} + (\epsilon_{\infty}^{-1} - \epsilon_0^{-1}) e^{-r/r_0}], \quad (30)$$

which is close to the well-known Haken potential¹⁴ and interpolates between the ϵ_0 exciton at low energies/large distances and the ϵ_{∞} exciton at high energies/small distances. The corresponding Green's function obeys

$$\left(E_{g0} - \frac{\hbar^2}{2\mu} \Delta_{\mathbf{r}} + V_H(r) - \hbar z \right) G_H(\mathbf{r}, \mathbf{r}'', z) = \delta(\mathbf{r} - \mathbf{r}''). \quad (31)$$

Obviously, the Haken potential fails to display any exciton-phonon resonance feature since it is basically a static quantity. However, it serves as a suitable starting point to solve the XPR problem. This is implemented by adding and subtracting the term (28) in Eq. (25)

$$\begin{aligned} & \left(E_{g0} - \frac{\hbar^2}{2\mu} \Delta_{\mathbf{r}} + V_H(r) - \hbar z \right) G(\mathbf{r}, \mathbf{r}'', z) - \sum_{\mathbf{q}} \int d\mathbf{r}' M_{\mathbf{q}}^*(\mathbf{r}) \\ & \times \left[G(\mathbf{r}, \mathbf{r}', z - \omega_0 - \omega_{\mathbf{q}}) - \frac{\delta(\mathbf{r} - \mathbf{r}')}{\hbar \omega_0 + \epsilon_{\mathbf{q}}} \right] M_{\mathbf{q}}(\mathbf{r}') G(\mathbf{r}', \mathbf{r}'', z) \\ & = \delta(\mathbf{r} - \mathbf{r}''). \end{aligned} \quad (32)$$

Writing the resolvent and the internal δ function as sum over states,¹⁹ we get

$$\begin{aligned} & \left(E_{g0} - \frac{\hbar^2}{2\mu} \Delta_{\mathbf{r}} + V_H(r) - \hbar z \right) G(\mathbf{r}, \mathbf{r}'', z) \\ & - \sum_{\mathbf{q}n} \int d\mathbf{r}' M_{\mathbf{q}}^*(\mathbf{r}) \phi_n^*(\mathbf{r}) \left[\frac{1}{\hbar \omega_0 + \epsilon_{\mathbf{q}} + \mathcal{E}_n - \hbar z} \right. \\ & \left. - \frac{1}{\hbar \omega_0 + \epsilon_{\mathbf{q}}} \right] \phi_n(\mathbf{r}') M_{\mathbf{q}}(\mathbf{r}') G(\mathbf{r}', \mathbf{r}'', z) = \delta(\mathbf{r} - \mathbf{r}''), \end{aligned} \quad (33)$$

where wave functions ϕ_n and eigenvalues \mathcal{E}_n refer to the *full* problem now. For weak coupling as applicable to GaAs, the first order perturbation theory with respect to the self-energy difference [sum over \mathbf{q} and n in Eq. (33)] is expected to work well. Then, combining Eqs. (13), (31), and (33) the response function is given approximately by

TABLE I. Semiconductor parameters used in the numerical calculations.

Parameter	CdTe	GaAs
ϵ_0	10.0 ^a	12.4 ^b
ϵ_{∞}	6.0 ^a	10.7 ^b
m_e/m_0	0.11 ^a	0.067 ^b
m_h/m_0	0.5 ^a	0.38 ^c
μ/m_0	0.064 ^d	0.046
$\hbar \omega_0$	21.0 meV ^a	36.7 meV ^b
R_0	10.0 meV ^a	4.0 meV ^b

^aReference 13.

^bReference 15.

^c $(m_h/m_0)^{-1} = \gamma_1 - 2\gamma_2$ with Luttinger parameters γ_1 and γ_2 .

^dFrom the fit (see text).

$$\begin{aligned} \chi(z) &= G_H(0,0,z) + \sum_{\mathbf{q}n} \int d\mathbf{r} M_{\mathbf{q}}^*(\mathbf{r}) G_H(0,\mathbf{r},z) \phi_n^*(\mathbf{r}) \\ & \times \left[\frac{1}{\hbar \omega_0 + \epsilon_{\mathbf{q}} + \mathcal{E}_n - \hbar z} - \frac{1}{\hbar \omega_0 + \epsilon_{\mathbf{q}}} \right] \\ & \times \int d\mathbf{r}' M_{\mathbf{q}}(\mathbf{r}') G_H(0,\mathbf{r}',z) \phi_n(\mathbf{r}'), \end{aligned} \quad (34)$$

where ϕ_n and \mathcal{E}_n have to be taken in *Haken* quality now. Further, a reduction of the sum to the dominant bound state $n=1s$ is expected to give the main resonance feature.

In Ref. 13 a similar expression for $\chi(z)$ using perturbation theory was obtained, but the result differs from Eq. (34) in two respects: the Coulomb Green's functions G_0 instead of G_H has been used, and the second term in the square bracket of Eq. (34) was missing. Our numerical calculations have shown that the first approximation is not a bad one since for weakly polar material the ‘‘Haken’’ quantities are rather close to the ‘‘static screened’’ ones (but differ markedly from the polaron-free case G_{∞}). However, the failure to subtract the second energy denominator would give a large change in the bound state region. In contrast, our procedure was chosen to give a small correction near $\mathcal{E}_{1s} = \hbar \omega$. This would not have been achieved using the original Haken potential¹⁴ which contains a sum of contributions with electron and hole polaron radii $r_{e,h} = \hbar/(2m_{e,h}\omega_0)$. In our framework, this potential form could be obtained by taking the free-particle Green's function instead of the high-frequency limit in Eq. (25).

VI. RESULTS AND COMPARISON WITH EXPERIMENT

We begin with CdTe where accurate absorption measurements at liquid nitrogen temperature have been reported some time ago by Dillinger *et al.*^{3,4} Details on the applied numerical procedures for the Green's function and the optical response can be found in the Appendix. The parameters used are listed in Table I. The valence band structure consists of heavy- and light-hole bands which are degenerate at the Γ point. Following Sak¹³ we adopt a simplified single-valence-band approximation with a density-of-states mass giving large weight to the heavy-hole component. We use this mass for the COM motion of the exciton. However, the internal

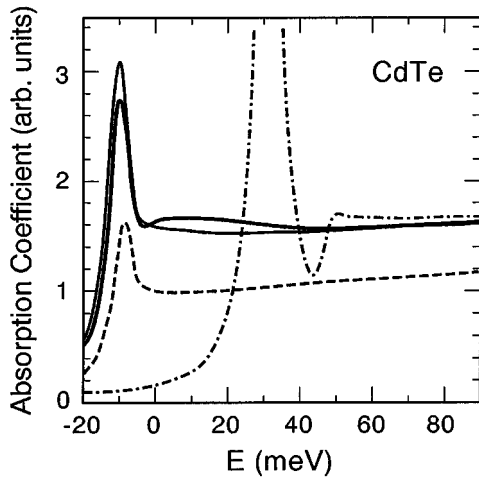


FIG. 2. Excitonic absorption $\alpha \sim \text{Im} \chi$ in bulk CdTe in dependence on energy $E = \hbar\omega - E_{g0}$. Calculated spectra for bare ϵ_∞ screening (dot-dashed curve), static ϵ_0 screening (dashed curve), with the Haken potential (thin solid curve), and full calculation including the XPR (thick solid curve). A Lorentz broadening of $\gamma = 4$ meV is used for all curves.

exciton motion is governed by the diagonal component of the Luttinger Hamiltonian (reduced effective mass $\mu^{-1} = m_e^{-1} + \gamma_1/m_0$, where γ_1 is the Luttinger parameter), which gives rise to degenerate heavy- and light-hole exciton states. We have chosen to use μ as an adjustable parameter for getting an exciton binding energy in agreement with the experimentally accepted value of $E_B = 10$ meV. We found $\mu = 0.064m_0$ resulting in a ϵ_0 -exciton binding energy $R_0 = 8.7$ meV which is then increased by the Haken potential towards the final 10 meV. Thus, even in the polar material CdTe, the difference between the ϵ_0 exciton and the Haken-screened exciton is not very large. This can be seen in Fig. 2 where the calculated exciton absorption $\alpha \sim \text{Im} \chi$ is displayed for the different levels of approximation. The hypothetical ϵ_∞ -exciton spectrum differs markedly by (missing) polaron shift, larger binding energy, and oscillator strength. Clearly seen is the interpolating character of the Haken spectrum which approaches the ϵ_∞ curve at large energies.

The dynamical exciton-LO contribution shows up as a broad feature on top of the Haken spectrum around the resonance energy $\mathcal{E}_{1s} + \hbar\omega_0 = E_{g0} + 11$ meV, but no clear structure is seen. This contrasts a simple Fano resonance argument where the interaction of a bound state with a continuum leads to a strong dispersive modification of the spectrum. But note that in the present case, the virtual state is a continuum, too, due to the COM dispersion $\mathcal{E}_{1s} + \hbar\omega_0 + \epsilon_Q$. We have checked that the overall Lorentz damping used ($\gamma = 4$ meV) is not responsible for the absence of sharp structures. Figure 3 shows the importance of taking the full continuum response [calculated from Eq. (33) with $n = 1s$] in comparison with the first order perturbation theory, Eq. (34). The structure is smeared out in the full calculation. The results shown in Fig. 2 for the excitonic absorption including the exciton-phonon resonance are in good agreement with the experimental data of Ref. 3 which are reproduced in Fig. 4.

In Fig. 5 we show the calculated exciton absorption for bulk GaAs using the different screening potentials. Here, an

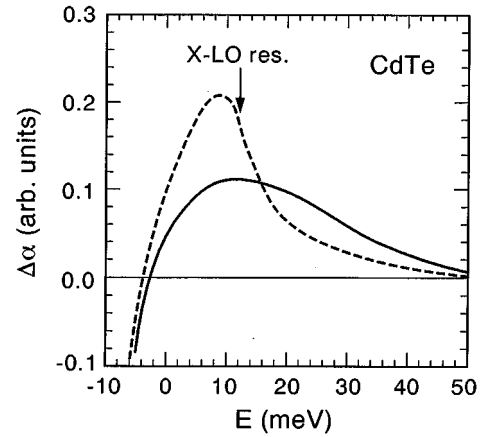


FIG. 3. Absorption difference $\Delta\alpha \sim \text{Im}[\chi(z) - \chi_H(z)]$ between the XPR and the Haken potential result for CdTe. First-order perturbation theory according to Eq. (34) (dashed curve) is compared with the full calculation, Eq. (33) (solid curve). The energetic position of the exciton-LO-phonon resonance is indicated by an arrow.

exciton reduced mass of $\mu = 0.046m_0$ follows from the Luttinger parameter $\gamma_1 = 6.85$. As in the CdTe case the statically (ϵ_0) screened exciton differs not much from the Haken case, whereas the bare exciton spectrum is displaced towards higher energies by the polaron shift. In GaAs the Fröhlich coupling parameter is very small and equal to 0.068 for electrons, so that the XPR causes only a rather weak spectral feature above the gap hardly visible in both the experimental

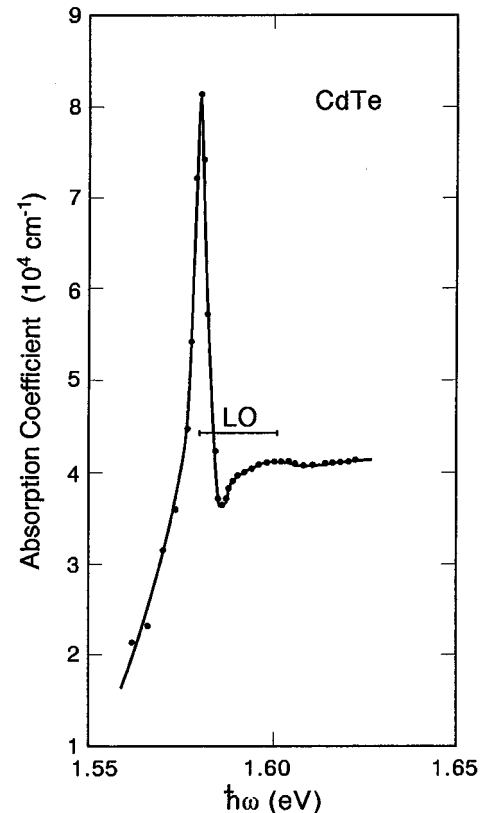


FIG. 4. Measured absorption coefficient of bulk CdTe at $T = 93$ K (after Ref. 3).

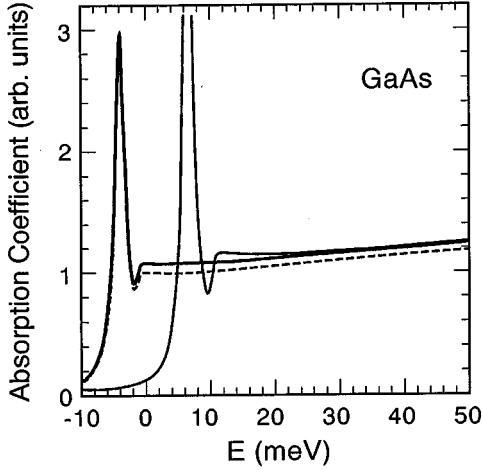


FIG. 5. Excitonic absorption $\alpha \sim \text{Im } \chi$ in bulk GaAs in dependence on energy $E = \hbar\omega - E_{g0}$. Calculated spectra are shown for bare ϵ_∞ screening (thin solid curve), static ϵ_0 screening (dashed curve), and with the Haken potential (thick solid curve). Lorentz broadening $\gamma = 1$ meV.

and calculated spectra. It can be seen more pronounced if we focus on the energy derivative of the absorption, $\alpha'(E)/\alpha(E)$. This spectrum is displayed in Fig. 6 for the Haken potential and the full result based on Eq. (34). The dynamical exciton-LO-phonon contribution shows up in a slight but rather abrupt change in the slope around the resonance energy $\mathcal{E}_{1S} + \hbar\omega_0$. Experimental absorption data for a 4.2 μm thick high-purity GaAs crystal have been numerically differentiated and are shown in Fig. 6 as circles.⁹ The XPR feature with its kink at 32.8 meV above the gap energy $E_{g0} = 1.5192$ eV compares well with the structure in the calculated spectrum, both in magnitude and energetic position. The overall slope of the experimental absorption curve is slightly larger. We believe that this is mainly due to the band nonparabolicity effect and/or heavy-light-hole valence band mixing in the exciton. Further, the smoothly varying reflec-

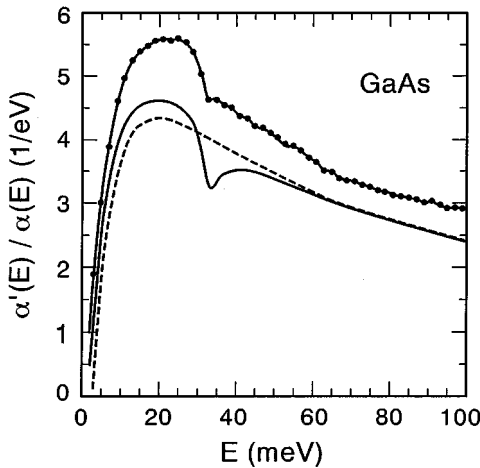


FIG. 6. Energy-derivative of the absorption, $\alpha'(E)/\alpha(E)$, in the excitonic continuum of GaAs. Circles—experiment at $T = 1.2$ K from Ref. 9, dashed curve—calculated with the Haken potential, solid curve—full calculation including the exciton-phonon resonance.

tance has not been corrected for in the experimental data.

In conclusion, we have developed a theoretical approach for the exciton-phonon resonance in the absorption coefficient above the gap in bulk semiconductors. Using an exciton Green's function formalism, the weak structure seen in the exciton continuum of several semiconductors has been shown to result from the interaction of continuum states with the virtual excitation of exciton ground state plus one LO phonon. We stress that the reformulation in terms of an effective Haken potential is necessary before using perturbation theory. The calculated excitonic absorption agrees well with experimental data for CdTe and GaAs. This good agreement between theory and experiment underlines that the present treatment gives a reliable description of the exciton continuum absorption in the vicinity of the exciton-phonon resonance.

ACKNOWLEDGMENTS

The authors gratefully acknowledge intense discussions with R. Ulbrich, who provided the experimental absorption data on GaAs. Part of this work has been supported by the exchange program between Humboldt University Berlin and University of Havana.

APPENDIX

Numerical procedures to calculate the exciton Green's function in real space have been developed earlier by one of the present authors.¹⁶ For the sake of completeness we present the relevant material in this Appendix, extending the treatment given in Ref. 16 to a *nonlocal* Schrödinger equation. Equation (33) is rewritten as

$$\left(E_{g0} - \frac{\hbar^2}{2\mu} \Delta_{\mathbf{r}} + V_H(r) - \hbar z \right) G(\mathbf{r}, \mathbf{r}', z) - \int d\mathbf{r}'' W(\mathbf{r}, \mathbf{r}'', z) G(\mathbf{r}'', \mathbf{r}', z) = \delta(\mathbf{r} - \mathbf{r}'), \quad (\text{A1})$$

with the kernel ($\alpha = m_h/M$, $\beta = m_e/M$),

$$W(\mathbf{r}, \mathbf{r}', z) = \sum_n \phi_n^*(\mathbf{r}) [w_n(\alpha\mathbf{r} - \alpha\mathbf{r}') + w_n(\beta\mathbf{r}' - \beta\mathbf{r}) - w_n(\alpha\mathbf{r} + \beta\mathbf{r}') - w_n(-\beta\mathbf{r} - \alpha\mathbf{r}')] \phi_n(\mathbf{r}'). \quad (\text{A2})$$

The integration over \mathbf{q} could be performed analytically yielding

$$w_n(\mathbf{r}) = \frac{e^2}{2\eta r} \left[\left(\frac{r_n}{r_0} \right)^2 (1 - e^{-r/r_n}) - (1 - e^{-r/r_0}) \right], \quad (\text{A3})$$

with the (complex and state dependent) polaron radii

$$r_n^2 = \frac{\hbar^2/2M}{\hbar\omega_0 + \mathcal{E}_n - \hbar z}. \quad (\text{A4})$$

A decomposition with respect to angular momentum reveals that, in general, different l components of the Green's function are coupled. However, if we restrict ourselves to $n = 1s$ as an intermediate state, the s component

$$G(\mathbf{r}, \mathbf{r}'', z)|_s = \frac{1}{4\pi r r''} g(r, r'', z) \quad (\text{A5})$$

obeys a closed equation which reads

$$\begin{aligned} \frac{\hbar^2}{2\mu} \frac{\partial^2 g(r, r'', z)}{\partial r^2} &= [E_{g0} + V_H(r) - \hbar z] g(r, r'', z) \\ &- 4\pi r \int_0^\infty dr' r' W(r, r', z) g(r', r'', z) \\ &- \delta(r - r''). \end{aligned} \quad (\text{A6})$$

Note that we have divided the Green's function by $(r r'')$ in order to remove the first-order derivative. The angular average in the kernel, $W(r, r', z) = \overline{W(\mathbf{r}, \mathbf{r}', z)}$, can be performed analytically with

$$\begin{aligned} \overline{w_n(\mathbf{r} - \mathbf{r}')} &= \frac{e^2}{2\eta r} \left[\frac{r_n^2}{r_0^2} - \frac{r_n^3}{r' r_0^2} e^{-r/r_n} \sinh(r'/r_n) - 1 \right. \\ &\left. + \frac{r_0}{r'} e^{-r/r_0} \sinh(r'/r_0) \right]. \end{aligned} \quad (\text{A7})$$

For $r < r'$, the variables r and r' have to be interchanged.

For the construction of the Green's function it is sufficient to determine two linearly independent solutions $X(r)$ and $Y(r)$ of the corresponding homogeneous equations [dropping the δ function in Eq. (A6)]. If $X(r)$ is chosen to be regular at the origin, and $Y(r)$ regular at infinity, the Green's function is given by

$$g(r, r'', z) = \frac{X(\min(r, r'')) Y(\max(r, r''))}{\mathcal{W}[Y, X]}, \quad (\text{A8})$$

with the Wronski determinant $\mathcal{W}[Y, X] = YX' - Y'X$. To simplify the expressions, we use from Eq. (A8) onwards units of the ϵ_0 exciton: Bohr radius $a_0 = \hbar^2 \epsilon_0 / (\mu e^2)$ and binding energy $R_0 = \hbar^2 a_0^2 / 2\mu$.

For the optical response [cf. Eq. (6)] we need the Green's function at zero arguments,

$$\chi(z) = \frac{1}{4\pi} \lim_{r \rightarrow 0} \frac{X(r) Y(r)}{r^2 \mathcal{W}[Y, X]}. \quad (\text{A9})$$

The series expansion of $X(r)$ and $Y(r)$ at small argument can be derived as

$$X(r) = r + \frac{a}{2} r^2 + O(r^3), \quad (\text{A10})$$

$$Y(r) = [A(z) + B(z)a \ln(r)] X(r) + B(z) + O(r^2). \quad (\text{A11})$$

The logarithmic term in the solution $Y(r)$ is due to the Coulomb singularity of the potential, here represented by the constant $a = -2\epsilon_0 / \epsilon_\infty$. The Wronskian equals $B(z)$, and plugging both expansions into Eq. (A9) gives as a final result

$$\chi(z) = \frac{1}{4\pi} \frac{A(z)}{B(z)}. \quad (\text{A12})$$

Additional terms have been dropped which are divergent. Being real and independent of frequency, they renormalize the background dielectric constant only (see Ref. 16 for a detailed explanation).

The coefficients $A(z)$ and $B(z)$ in $Y(r)$ [Eq. (A11)] contain all the information, they have to be determined after solving the integrodifferential equation

$$\begin{aligned} Y''(r) &= (E_{g0} + V_H(r) - \hbar z) Y(r) \\ &- 4\pi r \int_0^\infty dr' r' W(r, r', z) Y(r'). \end{aligned} \quad (\text{A13})$$

To do so we discretize the spatial variable in equidistant steps Δ . The second order derivative is often discretized by central differences as $Y''(r) = [Y(r + \Delta) + Y(r - \Delta) - 2Y(r)] / \Delta^2$. This simple form has an error of order Δ^2 , which can be markedly reduced by implementing

$$\begin{aligned} Y(r + \Delta) + Y(r - \Delta) - 2Y(r) &= \frac{\Delta^2}{12} [F(r + \Delta) + F(r - \Delta) \\ &+ 10F(r)], \end{aligned} \quad (\text{A14})$$

where $F(r)$ represents the rhs of Eq. (A13). The error of this so-called Numerov scheme²⁰ is of an order of Δ^4 and allows us to use a moderate step size. We found $\Delta = 0.04a_0$ to be sufficient. The size of the matrix equation (A14) scales with the maximum r value used. For calculating, e.g., the exciton ground state, a maximum of $r_1 = 4a_0$ is sufficient. However, to get a reliable absorption continuum well above the energy gap, a much larger cutoff is important (we have used $r_2 = 8a_0$). Additionally, the wave function has to be matched to the quasiclassical expression there,

$$Y(r_2) = 1,$$

$$\begin{aligned} Y(r_2 - \Delta) &= \sqrt{\kappa(r_2) / \kappa(r_2 - \Delta)} \\ &\times \exp\{\Delta[\kappa(r_2) + \kappa(r_2 - \Delta)]/2\}, \end{aligned} \quad (\text{A15})$$

where $\kappa^2(r) = [E_{g0} + V_H(r) - \hbar z] / R_0$. The nonlocal part $W(r, r', z)$, however, is practically zero above r_1 . Therefore, Eq. (A14) can be used recursively down to r_1 . Using Simpson's rule for the integral over r' in Eq. (A13), the remainder down to $r = \Delta$ can be treated as a linear matrix problem. Finally, fitting $Y(2\Delta)$ and $Y(\Delta)$ with the limiting expression (A11) provides the complex coefficients $A(z)$ and $B(z)$ needed to get the optical response from Eq. (A12).

For the ϵ_0 exciton with $V_0(r) = -2/r$, an analytic expression is obtained,²¹

$$\chi(z) = -\frac{1}{\pi} [\psi(1 - 1/\kappa) + \ln(\kappa) + \kappa/2], \quad (\text{A16})$$

with $\psi(x)$ being Euler's digamma function, and $\kappa^2 = (E_{g0} - \hbar z) / R_0$. Equation (A16) can be used to control the accuracy of the numerical procedure.

- ¹W. Y. Liang and A. D. Yoffe, Phys. Rev. Lett. **20**, 59 (1968).
- ²W. C. Walker, D. M. Roesler, and E. Loh, Phys. Rev. Lett. **20**, 847 (1968).
- ³Č. Koňák, J. Dillinger, and V. Prosser, in *Proceedings of the International Conference on II-VI Semiconductor Compounds*, edited by D. G. Thomas (Benjamin, New York, 1967), p. 850.
- ⁴J. Dillinger, Č. Koňák, V. Prosser, J. Sak, and M. Zvára, Phys. Status Solidi B **29**, 707 (1968).
- ⁵F. Iikawa, C. Trallero-Giner, and M. Cardona, Solid State Commun. **79**, 131 (1991).
- ⁶J. Lee, N. C. Giles, and C. J. Summers, Phys. Rev. B **49**, 11 459 (1994); J. Lee and N. C. Giles, J. Appl. Phys. **78**, 1191 (1995).
- ⁷F. H. Pollak, P. Ram, T. Holden, J. L. Freeouf, B. X. Yang, and M. C. Tamargo, in *Proceedings of the 23rd International Conference on the Physics of Semiconductors, Berlin, 1996*, edited by M. Scheffler and R. Zimmermann (World Scientific, Singapore, 1996), p. 289.
- ⁸A. Leitenstorfer, C. Fürst, A. Laubereau, W. Kaiser, G. Tränkle, and G. Weimann, Phys. Rev. Lett. **76**, 1545 (1996); A. Leitenstorfer and C. Fürst, in *Proceedings of the 23rd International Conference on the Physics of Semiconductors, Berlin, 1996*, edited by M. Scheffler and R. Zimmermann (World Scientific, Singapore, 1996), p. 661.
- ⁹C. Trallero-Giner, R. Zimmermann, M. Trinn, and R. Ulbrich, in *Proceedings of the 23rd International Conference on the Physics of Semiconductors, Berlin, 1996*, edited by M. Scheffler and R. Zimmermann (World Scientific, Singapore, 1996), p. 345.
- ¹⁰R. J. Elliott, Phys. Rev. **108**, 1384 (1957).
- ¹¹Y. Toyozawa and J. Hermanson, Phys. Rev. Lett. **21**, 1637 (1968); J. C. Hermanson, Phys. Rev. B **6**, 5043 (1970).
- ¹²L. Kalok and J. Treusch, Phys. Status Solidi B **52**, K115 (1972).
- ¹³K. Sak, Phys. Rev. Lett. **25**, 1654 (1970).
- ¹⁴H. Haken, Fortschr. Phys. **6**, 271 (1958); Nuovo Cimento **10**, 1230 (1956).
- ¹⁵C. Trallero-Giner, M. Cardona, and F. Iikawa, Phys. Rev. B **48**, 5187 (1993).
- ¹⁶R. Zimmermann, Phys. Status Solidi B **135**, 681 (1986).
- ¹⁷E. Haga, Prog. Theor. Phys. **13**, 555 (1955).
- ¹⁸I. B. Levinson and E. I. Rashba, Usp. Fiz. Nauk **111**, 687 (1973) [Sov. Phys. Usp. **16**, 892 (1974)].
- ¹⁹Strictly speaking the full Green's function has no resolvent expression with *real* eigenvalues. Later we use here only the exciton ground state of the Haken problem where no problems occur.
- ²⁰B. Numerov, Publ. Observ. Astrophys. Centre Russie No. 11, Moscow 1923.
- ²¹R. Zimmermann, Phys. Status Solidi B **159**, 317 (1990).